

Expression and Mutation of *SLC45A2* Affects Iris Color in Quail

Linke Huo¹, Xiaohui Zhang^{1,2}, Youzhi Pang^{1,2}, Yanxia Qi^{1,2}, Shiwei Ren¹, Fanghu Wu¹,
Yuanyuan Shang¹ and Jinqian Xi¹

¹College of Animal Science, Henan University of Science and Technology, Luoyang, 471003 He'nan, P.R. China

²Luoyang Key Laboratory of Animal Genetics and Breeding, Luoyang 471003, P.R. China

Iris color is a prominent phenotypic feature of quail. To understand the mechanism of melanin deposition related to quail iris color, iris tissues were selected from Beijing white and Chinese yellow quail for transcriptome analysis. Differentially expressed genes (DEGs) associated with pigmentation were identified using RNA sequencing and validated by quantitative real-time polymerase chain reaction (RT-qPCR). The identified single nucleotide polymorphisms were studied using bioinformatics and iris color correlation analyses. A total of 485 DEGs were obtained, with 223 upregulated and 262 downregulated. Gene ontology (GO) and Kyoto Encyclopedia of Genes and Genomes pathway enrichment analyses were performed. Thirty-two genes were annotated using the GO database. Three important pigment synthesis pathways (Notch signaling, melanogenesis, and tyrosine metabolism) were identified in quail iris tissue ($P < 0.05$). The expression levels of solute carrier family 45 member 2 (*SLC45A2*), tyrosinase-related protein 1, vitamin D receptor, opsin 5, and docking protein 5 were significantly different between Beijing white and Chinese yellow quail, as verified by RT-qPCR. The c.1061C>T mutation in *SLC45A2*, which caused a single amino acid change at position 354 (threonine to methionine), was significantly associated with iris color in Beijing white and Chinese yellow quail, and might be the main reason for the different iris colors between these two quail species.

Key words: iris color, quail, RNA-Seq, RT-qPCR, *SLC45A2*

J. Poultry Sci., 61: jpsa.2024015, 2024

Introduction

Iris color is one of the most prominent phenotypic features in birds[1]. Some birds have bright yellow, red, or white irises, which may be related to their behavior, breeding strategies, or environmental adaptability[2,3]. However, some birds have dark irises, which may help improve visual acuity or help them adapt to specific habitats[4]. As an ancient bird species, quails have exhibited a wide range of iris color variations throughout their evolutionary history[5]. In recent years, quails have gained widespread attention and importance as a highly productive poultry species. Current research on quails mainly focuses on exploring genetic patterns and practical applications related to feather color[6]. However, there are few reports on the mechanisms

underlying iris color deposition in quails. In the eyes of quails, melanocytes are located in the anterior part of the iris and melanin production determines iris color[7]. The amount of melanin directly affects iris color. Generally, the more melanin there is, the darker the iris color; conversely, the lighter the iris color, the less melanin[8]. Beijing white quail are a mutant strain of Korean quail (chestnut-colored feathers) with bright pink eyes (Fig. 1). Genes have a significant effect on melanin production and distribution in the iris[9]. Melanin production is controlled by multiple genes, including tyrosinase-related protein 1 (*TYRP1*), melanocortin 1 receptor, and oculocutaneous albinism type 2[10]. Variations in single-nucleotide polymorphisms (SNPs) significantly affect the phenotypic coloration of organisms[11]. RNA sequencing (RNA-Seq) was performed on embryonic iris tissues of Beijing white and Chinese yellow quail, followed by quantitative real-time PCR (RT-qPCR) validation. Differentially expressed genes (DEGs) related to iris pigment deposition in quails were identified. To explore the association between solute carrier family 45 member 2 (*SLC45A2*) gene polymorphisms and iris color in different quail breeds, the relationship between the c.1601C>T mutation site in the *SLC45A2* gene and iris color traits was analyzed. Revealing the genetic mechanisms underlying

Received: January 22, 2024, Accepted: May 9, 2024

Available online: May 30, 2024

Correspondence: Dr. Xiaohui Zhang, College of Animal Science, Henan University of Science and Technology, 263 Kaiyuan Avenue, Luoyang, China. (E-mail: zhangxiaohui78@126.com)

The Journal of Poultry Science is an Open Access journal distributed under the Creative Commons Attribution-NonCommercial-Share-Alike 4.0 International License. To view the details of this license, please visit (<https://creativecommons.org/licenses/by-nc-sa/4.0/>).

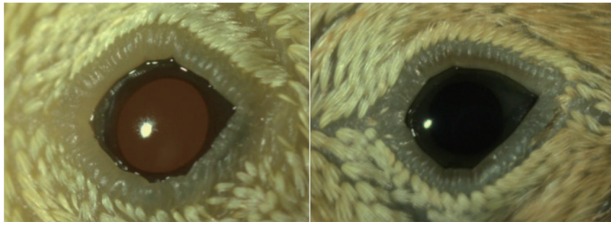


Fig. 1. Beijing white quail iris (Left) and Chinese yellow quail iris (Right).

ing iris color in quail has important implications for quail development and breeding.

Materials and Methods

Sample collection

Fertilized eggs of Beijing white and Chinese yellow quails were obtained from the Poultry Research Center of Henan University of Science and Technology (HAUST). Tissue samples for RNA-Seq and RT-qPCR were collected from the irises of four embryos of each breed at embryonic day 10 (E10). Blood samples from 299 Beijing white and 298 Chinese yellow quail were collected from the Poultry Research Center of HAUST. All experimental surgical procedures were approved by the Biological Studies Animal Care and Use Committee of Henan Province (approval number: HAUST (2020) -19).

Sequencing data quality assessment and mapping

Clean reads were obtained by quality control of raw data using Cutadapt (version 2.4), including the removal of junctions, duplicate sequences, and low-quality sequences. FastQC (version 0.11.8) was used to check the quality of clean reads.

Clean reads were mapped to the quail reference genome (GCF_001577835.2) using the HISAT2 software (version 2.0.4)

to obtain information on their location and sample-specific sequence characteristics. SAMtools (version 0.1.18) was used for sorting and format conversion to BAM files, and Picard (version 2.21.6) was used to remove PCR duplicates.

StringTie (version 2.1.2) was used to normalize gene expression and qualified data were analyzed for expression. The fragments per kilobase of transcript per million mapped reads value of each gene in each sample was calculated using the RSEM (version 1.2.15) software.

Screening and analysis of DEGs

DEGs were analyzed using the R package edgeR (version 4.1) and the *P* value and false discovery rate (FDR) values of DEGs were calculated. DEGs were identified according to $FDR < 0.05$, and \log_2 fold change > 1 . The ggplot2 package in R was used to draw a DEG volcano plot. DEGs were subjected to gene ontology (GO) functional analysis and Kyoto Encyclopedia of Genes and Genomes (KEGG) pathway analysis using the Database for Annotation, Visualization and Integrated Discovery (version 6.8). The calculated *P*- values were corrected using the Benjamini-Hochberg correction and enriched terms were considered statistically different when the adjusted $P < 0.05$.

RT-qPCR verification

Using eukaryotic translation initiation factor 2 subunit 3 (*EIF2S3*)[12] as the internal reference gene, RT-qPCR was used to detect the expression levels of the *SLC45A2* gene in E10 embryos of Beijing white and Chinese yellow quail. *SLC45A2* and *EIF2S3* primers were designed using Primer 5.0 software (Table 1), which were synthesised by Beijing Tsingke Biotech Co., Ltd. The RT-qPCR reaction system (20 μ L) consisted of 1 μ L of cDNA template, 10 μ L SYBR Premix Ex Taq™ II (2 \times) (Takara, Dalian, China), 0.7 μ L forward primers, 0.7 μ L reverse primers, and 7.6 μ L ddH₂O (Takara). The RT-qPCR reaction conditions were as follows: pre-denaturation at 95 $^{\circ}$ C for 3 min, denaturation at 95 $^{\circ}$ C for 20 s, annealing for 30 s (the annealing temperature of each

Table 1. KASP and qPCR primers

Gene	Primer sequences (5' \rightarrow 3')	Product length(bp)	Annealing temperature($^{\circ}$ C)	Purpose
<i>SLC45A2</i>	F: GAAGGAACAAGGCACAGA R: AGCAACACTGACCAAGAG	121	58	qPCR
<i>TYRP1</i>	F:ACACTCCTCTTTTATTCC R:TTTGCCCTCCTGTTCCATTC	144	59.8	qPCR
<i>VDR</i>	F: CAGAGGAAGCGTGAGATG R: GAGGAGGATGTTGATGACTT	108	75.7	qPCR
<i>OPN5</i>	F: CCGTTGAATGGTTGAGAAG R: GAAGTGGATGGTGTGCTAT	170	72.1	qPCR
<i>DOK5</i>	F: TAACTGCTGGCTGGTATTC R: CTACACTTGCTCCTTATTGC	155	72.5	qPCR
<i>EIF2S3</i>	F:GATTGACCCAACCTTGTGCC R:TTCTTGCTCCTTCAGTGCG	147	60	qPCR
<i>SLC45A2</i> (c.1061C>T)	F: TGTTTTTAGGCTCAAAGGCG	156	59	KASP

NOTE: KASP, kompetitive allele-specific polymerase chain reaction; qPCR, quantitative polymerase chain reaction; *SLC45A2*, solute carrier family 45 member 2; *TYRP1*, tyrosinase-related protein 1; *VDR*, vitamin D receptor; *OPN5*, opsin 5; *DOK5*, docking protein 5; *EIF2S3*, eukaryotic translation initiation factor 2 subunit 3.

gene is shown in Table 1), and extension at 72 °C for 20 s (40 cycles); fluorescence signals were collected during the extension phase. The melting curve was increased by 0.5 °C every 5 s from 65–95 °C. The relative expression of genes was calculated using the $2^{-\Delta\Delta Ct}$ method.

Polymorphism detection

SNPs in *SLC45A2* were identified using RNA-Seq data. SNP calling was performed using GATK (version 4.3.0), and SNP annotation was performed using SnpEff (version 5.2). The *SLC45A2* gene sequence of Japanese quail (NM_001083364.3) was downloaded from the GenBank database. One pair of primers (one positive primer and two negative primers) was designed using the Primer 5.0 software (Table 1), which were synthesised by Beijing Tsingke Biotech Co., Ltd. The c.1061C>T site in the *SLC45A2* gene of Beijing white and Chinese yellow quail was genotyped using kompetitive allele-specific PCR (KASP) technology. The KASP reaction system conditions were as follows: KASP 2× Master mix V3 (5 µL) (LGC Genomics, London, UK), forward universal primer F (0.9 µL), reverse typing primer R1 (0.3 µL), reverse typing primer R2 (0.3 µL), template DNA (1 µL), and ddH₂O (2.5 µL) (Takara); the total volume was 10 µL. The reaction conditions were as follows: the first step was at 94 °C for 6 min; the second step was denaturation at 94 °C for 20 s, annealing at 61 °C for 60 s, 10 cycles; the third step was denaturation at 94 °C for 20 s, annealing at 59 °C for 60 s, 26 cycles; and the fourth step was at 37 °C for 5 min (KASP typing data should generally be read below 40 °C). The amplified products were analyzed using an RT-qPCR instrument (Bio-Rad, Hercules, CA, USA) to obtain the relative fluorescence unit values for each sample. Genotyping was performed using R, version 4.1.2, and the ggplot2 package.

Statistical analysis

The gene expression data of the two quail varieties were used for Student's *t*-test analysis using SPSS (version 17.0) and GraphPad Prism (version 8.0) for graphing. Polymorphic information content (PIC), allele, and genotype frequencies were directly calculated using Cervus (version 3.0). The chi-squared test (χ^2) was used to determine whether the populations were in Hardy-Weinberg equilibrium (HWE).

Results

RNA-Seq

RNA-Seq data obtained for each sample ranged from 6.64–7.17 G. The Q30% ranged from 93.49%–94.52%, with an average GC content of 49.39%. The mapping rate was 88.53%–90.49%.

Analysis of DEGs

A total of 485 DEGs were identified, of which 223 were up-regulated and 262 were downregulated in iris tissues of Beijing white quail (Fig. 2). Thirty-two genes were annotated in the GO database and 13 taxonomic entries were significantly enriched, with seven entries annotated as biological processes, five entries annotated as cellular components, and one entry annotated as a molecular function. There were 32 DEGs enriched in 8 KEGG

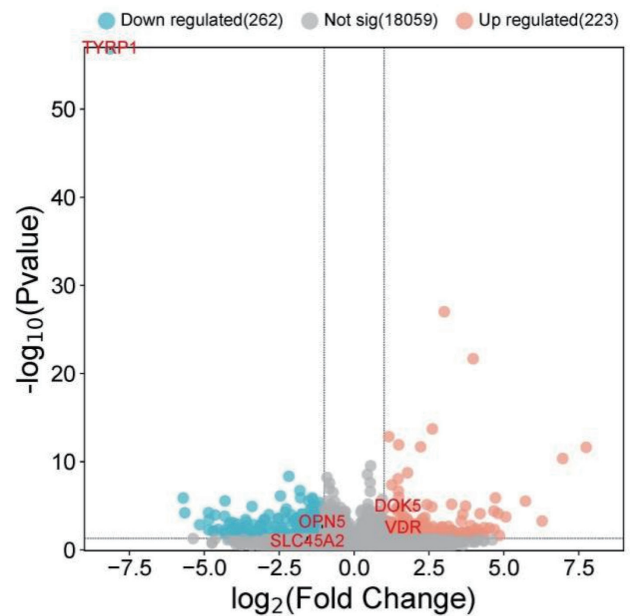


Fig. 2. Volcano plot of differentially expressed genes (DEGs).

pathways. Neuroactive ligand-receptor interaction was the most enriched pathway, followed by tight junctions, sphingolipid metabolism, and lysosomes. KEGG enrichment analysis showed that three pathways (melanogenesis, the mitogen-activated protein kinase (MAPK) signaling pathway, and tyrosine metabolism) were significantly associated with iris color ($P < 0.05$). Through analysis and literature review, it was evident that the significant DEGs included genes associated with melanin synthesis, such as *SLC45A2*, *TYRP1*, vitamin D receptor (*VDR*), opsin 5 (*OPN5*), and docking protein 5 (*DOK5*). These genes play crucial roles in regulating melanin synthesis[13–17]

RT-qPCR verification

RT-qPCR was performed to validate the expression of the selected DEGs in the irises of Beijing white and Chinese yellow quail. The results are shown in Fig. 3. The expression levels of *SLC45A2*, *TYRP1*, *VDR*, *OPN5*, and *DOK5* in the iris of Chinese yellow quail were significantly different from those in Beijing white quail. Gene expression validated by RT-qPCR was consistent with the RNA-Seq results, thus validating the accuracy of the RNA-Seq data.

Genotypic analysis of the c.1061C>T mutation in *SLC45A2*

The c.1061C>T mutation was identified in exon 4 of *SLC45A2* and there were three genotypes at this mutation site (CC, CT, and TT). The dominant allele of the c.1061C>T locus was T in both quail populations. The PIC value for the c.1061C>T locus was 0.29, indicating that the mutant locus was moderately polymorphic ($0.25 < PIC < 0.5$). The c.1061C>T locus showed a χ^2 value of 0.66 and a *P*-value of 0.42 ($P > 0.05$); therefore the quail populations were in HWE at this mutant locus.

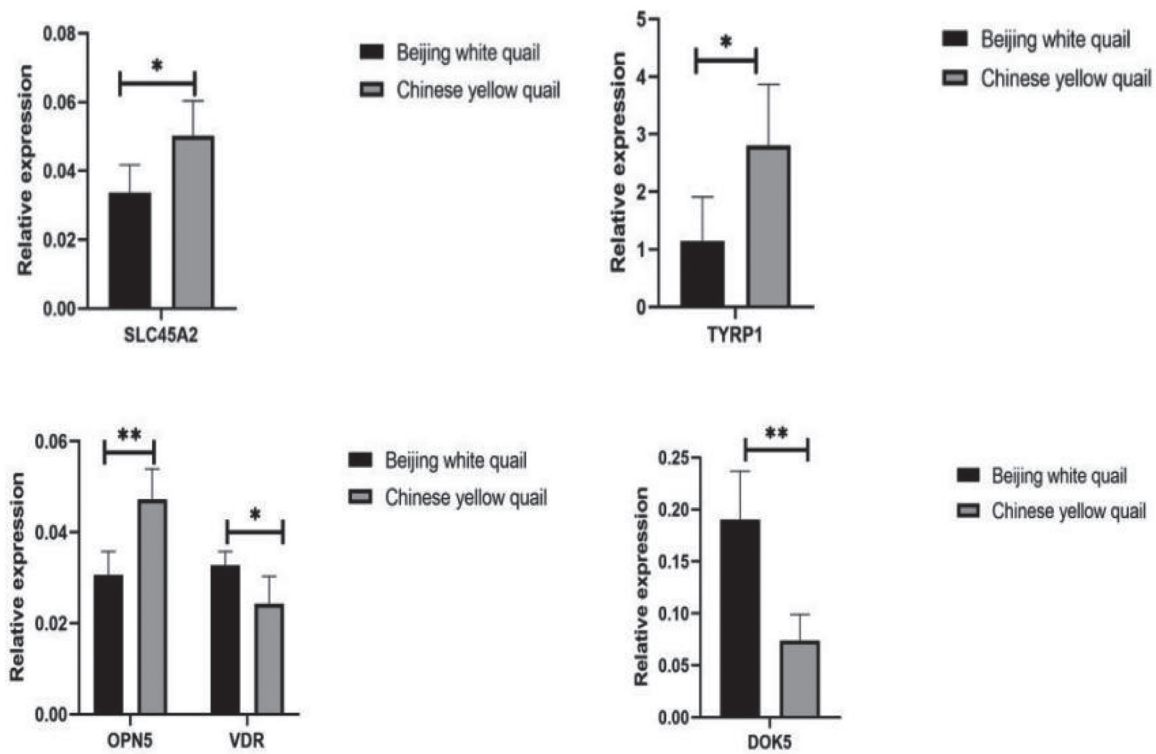


Fig. 3. **Relative expression of each candidate gene.** * indicates significant difference ($P < 0.05$); ** indicates highly significant difference ($P < 0.01$). *SLC45A2*, solute carrier family 45 member 2; *TYRP1*, tyrosinase-related protein 1; *VDR*, vitamin D receptor; *OPN5*, opsin 5; *DOK5*, docking protein 5.

Table 2. **Association between *SLC45A2* gene polymorphism and iris color in quails.**

Locus	phenotype	Total number	Genotype frequency			Allele frequencies		χ^2	P
			CC	CT	TT	C	T		
c.1061C>T	HF	298	0.06(19)	0.42(125)	0.52(154)	0.27	0.73	8.06	0.00
	BF	299	0.04(11)	0.46(138)	0.50(150)	0.27	0.73		

NOTE: *SLC45A2*, solute carrier family 45 member 2; BF, Beijing white quail; HF, Chinese yellow quail.

Correlation of gene mutations with iris color

The frequency distribution of c.1061C>T in Beijing white quail differed significantly from that in Chinese yellow quail. This indicated a significant association between the c.1061C>T mutation locus and iris color traits in quail ($P < 0.01$) (Table 2).

Functional analysis for *SLC45A2*

The biological information showed that the c.1061C>T mutation in *SLC45A2* could change the structure of the membrane protein, as this mutation caused the amino acid threonine (Thr) at position 354 in *SLC45A2* to be replaced by methionine (Met).

Discussion

Currently, research on quail body color primarily focuses on investigating the genetic patterns and practical applications of feather color[6]. There is limited research on the mechanism of

iris color deposition in quails. In this study, 485 DEGs were identified using RNA-Seq. Among these DEGs, *SLC45A2*, *TYRP1*, *VDR*, *OPN5*, and *DOK5* were most closely related to iris color formation, based on a comparison with other studies. Previous studies have shown that these genes are involved in avian color formation. *SLC45A2* is a transporter protein that is mainly expressed in pigment cells[18]. Its expression varies with different feather colors of Bashang long-tailed chickens, and its expression increases in melanocytes after the addition of tyrosine, indicating its involvement in feather color formation through the regulation of melanin production[13]. Mutations in *SLC45A2* are also the genetic basis for feather color in Japanese quails[19]. The *SLC2A11B* gene family, which is closely related to iris color in domestic pigeons, may also be a potential research direction to understand the mechanism of iris color formation in Beijing

white quails[1]. *TYRP1* is an enzyme involved in melanin biosynthesis and a decrease in *TYRP1* expression may lead to the formation of black feathers in Korean quails[20]. The *TYRP1* signaling pathway is crucial for the formation of black and white feathers in Japanese quail[21]. *TYRP1* is also an important gene involved in the formation of head feather color in mallards[14]. *OPN5* is a member of the G protein-coupled receptor opsin family that regulates the expression of *TYR*, *TYRP1*, and *TYRP2* through a calcium-dependent signaling pathway[22]. The quail *OPN5* and rat *OPN5* genes are involved in Ca^{2+} signaling cascades[23]. Ca^{2+} signaling is involved in melanin production in melanocytes, and *OPN5* is associated with hair color traits in vertebrates[15,24]. *VDR* is essential for the development of human choroidal melanocytes and melanin levels in choroidal melanoma negatively correlate with *VDR* expression[16]. *DOK5* is involved in neural signal transduction and encodes a protein that interacts with phosphorylated receptor tyrosine kinases, which mediate the growth of neural processes and activation of the MAPK pathway[25,26]. This pathway is involved in melanoma growth, invasion, and metastasis[27,28]. Wang[17] has observed that *DOK5* leads to abnormal melanin transfer in Liancheng white ducks, resulting in feather whitening, and that its polymorphism is also associated with feather color.

In Beijing white quails, *SLC45A2* expression was lower than that in other wild-type quails. Variations in this gene affect the expression of the *TYR* gene family in Beijing white quail[19]. However, the precise localization and specific regulatory mechanisms before and after gene variation remain unknown. *SLC45A2* belongs to the proton/sugar symport protein family and regulates pH by mediating H^+ to affect melanin synthesis[29,30]. This gene mutation leads to the mislocalization of *TYR* from melanosomes to the plasma membrane and the incorporation of *TYR* into exosomes[31]. This causes changes in feather color in chickens and Japanese quail, and red jungle fowl have abnormal melanin deposition, resulting in red eyes. Mutations in *SLC45A2* causing *OCA4* in vertebrates result in insufficient pigmentation in the skin, hair, and irises[32,33].

Transcriptome analysis of iris tissues with different plumage colors revealed that *VDR* and *DOK5* were upregulated in Beijing white quail, whereas *SLC45A2*, *TYRP1*, and *OPN5* were downregulated. *TYRP1* showed differential expression in the α -melanocyte stimulating hormone regulatory pathway between Beijing white and Chinese yellow quail, suggesting that differential expression of *TYRP1* may be involved in the regulation of iris color formation in Beijing white quail. The results of this study indicate that downregulation of *SLC45A2*, *TYRP1*, and *OPN5* may contribute to iris color formation in Beijing white quail, which is inconsistent with a few previous studies. Therefore, further validation and analyses are required. The DEGs identified in this study, many of which have unknown functions, provide a reference for further research on quail iris color.

A missense mutation, c.1061C>T, was detected in *SLC45A2*. Pearson's Chi-square test showed that Beijing white and Chinese yellow quail were in HWE at this locus. The frequency distribu-

tion of the CC, CT, and TT genotypes at the c.1061C>T locus in Chinese yellow quail was significantly different from that in Beijing white quail, indicating that this locus was associated with quail iris color. According to bioinformatics predictions, the c.1061C>T mutation caused by this locus was conserved and could lead to p.Thr354Met, thereby interfering with the conformational change and glycosylation function of the protein structure, which might be the main reason for the different iris colors between these two quail species.

In conclusion, five candidate genes (*SLC45A2*, *TYRP1*, *VDR*, *OPN5*, and *DOK5*) related to iris color were identified using RNA-Seq. The c.1061C>T mutation in *SLC45A2* was significantly correlated with iris color in quails. These findings provide a reference to study the molecular mechanisms of iris color traits in quails.

Acknowledgments

This study was supported by a Grant-in-Aid for Scientific Research from the Natural Science Foundation of Henan Province (grant number 202300410153).

Author Contributions

Linke Huo and Shiwei Ren conducted the experiments; Xiaohui Zhang designed the experiments; Yanxia Qi and Youzhi Pang analyzed and interpreted the data. Fanghu Wu, Yuanyuan Shang, and Jinquan Xi collected samples and performed the experiments. Linke Huo, Xiaohui Zhang, Yanxia Qi, Youzhi Pang, Shiwei Ren, Fanghu Wu, Yuanyuan Shang and Jinquan Xi drafted the manuscript.

Conflicts of Interest

The authors declare no conflict of interest.

References

- [1] Si S, Xu X, Zhuang Y, Gao X, Zhang H, Zou Z and Luo SJ. The genetics and evolution of eye color in domestic pigeons (*Columba livia*). *PLoS Genet*, **17**: e1009770. 2021. <https://doi.org/10.1371/journal.pgen.1009770>, PMID:34460822
- [2] Wu N, Gu T, Lu L, Cao Z, Song Q, Wang Z, Zhang Y, Chang G, Xu Q and Chen G. Roles of miRNA-1 and miRNA-133 in the proliferation and differentiation of myoblasts in duck skeletal muscle. *J Cell Physiol*, **234**: 3490–3499. 2019. <https://doi.org/10.1002/jcp.26857>, PMID:30471101
- [3] Maclary ET, Phillips B, Wauer R, Boer EF, Bruders R, Gilvarry T, Holt C, Yandell M and Shapiro MD. Two genomic loci control three eye colors in the domestic pigeon (*Columba livia*). *Mol Biol Evol*, **38**: 5376–5390. 2021. <https://doi.org/10.1093/molbev/msab260>, PMID:34459920
- [4] Davidson GL, Thornton A and Clayton NS. Evolution of iris colour in relation to cavity nesting and parental care in passerine birds. *Biol Lett*, **13**: 20160783. 2017. <https://doi.org/10.1098/rsbl.2016.0783>, PMID:28077686
- [5] Jurkevich A, Grossmann R, Balthazart J and Viglietti-Panzica C. Gender-related changes in the avian vasotocin system during ontogeny. *Microsc Res Tech*, **55**: 27–36. 2001. <https://doi.org/10.1002/jemt.1153>, PMID:11596147

- [6] Wu Y, Zhang Y, Hou Z, Fan G, Pi J, Sun S, Chen J, Liu H, Du X, Shen J, Hu G, Chen W, Pan A, Yin P, Chen X, Pu Y, Zhang H, Liang Z, Jian J, Zhang H, Wu B, Sun J, Chen J, Tao H, Yang T, Xiao H, Yang H, Zheng C, Bai M, Fang X, Burt DW, Wang W, Li Q, Xu X, Li C, Yang H, Wang J, Yang N, Liu X and Du J. Population genomic data reveal genes related to important traits of quail. *Gigascience*, **7**: gjy049. 2018. <https://doi.org/10.1093/gigascience/giy049>, PMID:29762663
- [7] Hu DN, Simon JD and Sarna T. Role of ocular melanin in ophthalmic physiology and pathology. *Photochem Photobiol*, **84**: 639–644. 2008. <https://doi.org/10.1111/j.1751-1097.2008.00316.x>, PMID:18346089
- [8] Oliphant LW, Hudon J and Bagnara JT. Pigment cell refugia in homeotherms--the unique evolutionary position of the iris. *Pigment Cell Res*, **5**: 367–371. 1992. <https://doi.org/10.1111/j.1600-0749.1992.tb00564.x>, PMID:1492070
- [9] Pośpiech E, Draus-Barini J, Kupiec T, Wojas-Pelc A and Branicki W. Gene–gene interactions contribute to eye colour variation in humans. *J Hum Genet*, **56**: 447–455. 2011. <https://doi.org/10.1038/jhg.2011.38>, PMID:21471978
- [10] Ishishita S, Takahashi M, Yamaguchi K, Kinoshita K, Nakano M, Nunome M, Kitahara S, Tatsumoto S, Go Y, Shigenobu S and Matsuda Y. Nonsense mutation in PMEL is associated with yellowish plumage colour phenotype in Japanese quail. *Sci Rep*, **8**: 16732. 2018. <https://doi.org/10.1038/s41598-018-34827-4>, PMID:30425278
- [11] Zhang X, Qi Y, Pang Y, Yuan B and Li X. Identification of polymorphisms in the *HERC2-OCA2* gene locus and their association with feather color in quail. *J Poult Sci*, **60**: 2023013. 2023. <https://doi.org/10.2141/jpsa.2023013>, PMID:37234755
- [12] Yuan ZW, Zhang XH, Pang YZ, Qi YX, Wang QK, Ren SW, Hu YQ, Zhao YW, Wang T and Huo LK. Screening of stably expressed internal reference genes for quantitative real-time PCR analysis in quail. *Biol Bull Russ Acad Sci*, **49**: 418–427. 2022. <https://doi.org/10.1134/S1062359022050223>
- [13] Liu X, Zhou R, Peng Y, Zhang C, Li L, Lu C and Li X. Hair follicles transcriptome profiles in Bashang long-tailed chickens with different plumage colors. *Genes Genomics*, **41**: 1357–1367. 2019. <https://doi.org/10.1007/s13258-018-0740-y>, PMID:30229509
- [14] Ma S, Liu H, Wang J, Wang L, Xi Y, Liu Y, Xu Q, Hu J, Han C, Bai L, Li L and Wang J. Transcriptome analysis reveals genes associated with sexual dichromatism of head feather color in mallard. *Front Genet*, **12**: 627974. 2021. <https://doi.org/10.3389/fgene.2021.627974>, PMID:34956302
- [15] Bellono NW, Kammel LG, Zimmerman AL and Oancea E. UV light phototransduction activates transient receptor potential A1 ion channels in human melanocytes. *Proc Natl Acad Sci USA*, **110**: 2383–2388. 2013. <https://doi.org/10.1073/pnas.1215555110>, PMID:23345429
- [16] Markiewicz A, Brożyna AA, Podgórska E, Elas M, Urbańska K, Jetten AM, Slominski AT, Józwicki W, Orłowska-Heitzman J, Dyduch G and Romanowska-Dixon B. Vitamin D receptors (VDR), hydroxylases CYP27B1 and CYP24A1 and retinoid-related orphan receptors (ROR) level in human uveal tract and ocular melanoma with different melanization levels. *Sci Rep*, **9**: 9142. 2019. <https://doi.org/10.1038/s41598-019-45161-8>, PMID:31235702
- [17] Wang L, Yang L, Yang S, Jia Z, Cai J, Rong L, Wu X, Fan L, Gong Y and Li S. Identification of genes associated with feather color in Liancheng white duck using F_{ST} analysis. *Anim Genet*, **53**: 518–521. 2022. <https://doi.org/10.1111/age.13201>, PMID:35670225
- [18] Le L, Escobar IE, Ho T, Lefkovith AJ, Latteri E, Haltaufderhyde KD, Dennis MK, Plowright L, Sviderskaya EV, Bennett DC, Oancea E and Marks MS. SLC45A2 protein stability and regulation of melanosome pH determine melanocyte pigmentation. *Mol Biol Cell*, **31**: 2687–2702. 2020. <https://doi.org/10.1091/mbc.E20-03-0200>, PMID:32966160
- [19] Gunnarsson U, Hellström AR, Tixier-Boichard M, Minvielle F, Bed'hom B, Ito S, Jensen P, Rattink A, Vereijken A and Andersson L. Mutations in SLC45A2 cause plumage color variation in chicken and Japanese quail. *Genetics*, **175**: 867–877. 2007. <https://doi.org/10.1534/genetics.106.063107>, PMID:17151254
- [20] Xu Y, Zhang XH and Pang YZ. Association of tyrosinase (TYR) and tyrosinase-related protein 1 (TYRP1) with melanic plumage color in Korean quails (*Coturnix coturnix*). *Asian-Australas J Anim Sci*, **26**: 1518–1522. 2013. <https://doi.org/10.5713/ajas.2013.13162>, PMID:25049736
- [21] Nadeau NJ, Mundy NI, Gourichon D and Minvielle F. Association of a single-nucleotide substitution in *TYRP1* with *roux* in Japanese quail (*Coturnix japonica*). *Anim Genet*, **38**: 609–613. 2007. <https://doi.org/10.1111/j.1365-2052.2007.01667.x>, PMID:18028514
- [22] Lan Y, Zeng W, Dong X and Lu H. Opsin 5 is a key regulator of ultraviolet radiation-induced melanogenesis in human epidermal melanocytes. *Br J Dermatol*, **185**: 391–404. 2021. <https://doi.org/10.1111/bjd.19797>, PMID:33400324
- [23] Sugiyama T, Suzuki H and Takahashi T. Light-induced rapid Ca²⁺ response and MAPK phosphorylation in the cells heterologously expressing human OPN5. *Sci Rep*, **4**: 5352. 2014. <https://doi.org/10.1038/srep05352>, PMID:24941910
- [24] Wicks NL, Chan JW, Najera JA, Ciriello JM and Oancea E. UVA phototransduction drives early melanin synthesis in human melanocytes. *Curr Biol*, **21**: 1906–1911. 2011. <https://doi.org/10.1016/j.cub.2011.09.047>, PMID:22055294
- [25] Sun P, Li R, Meng Y, Xi S, Wang Q, Yang X, Peng X and Cai J. Introduction of DOK2 and its potential role in cancer. *Physiol Res*, **70**: 671–685. 2021. <https://doi.org/10.33549/physiolres.934710>, PMID:34505522
- [26] Zhang LQ, Cui H, Yu YB, Shi HQ, Zhou Y and Liu MJ. MicroRNA-141-3p inhibits retinal neovascularization and retinal ganglion cell apoptosis in glaucoma mice through the inactivation of Docking protein 5-dependent mitogen-activated protein kinase signaling pathway. *J Cell Physiol*, **234**: 8873–8887. 2019. <https://doi.org/10.1002/jcp.27549>, PMID:30515784
- [27] Guo YJ, Pan WW, Liu SB, Shen ZF, Xu Y and Hu LL. ERK/MAPK signalling pathway and tumorigenesis (Review). *Exp Ther Med*, **19**: 1997–2007. 2020. <https://doi.org/10.3892/etm.2020.8454>, PMID:32104259
- [28] Najafi M, Ahmadi A and Mortezaee K. Extracellular-signal-regulated kinase/mitogen-activated protein kinase signaling as a target for cancer therapy: an updated review. *Cell Biol Int*, **43**: 1206–1222. 2019. <https://doi.org/10.1002/cbin.11187>, PMID:31136035
- [29] Dooley CM, Schwarz H, Mueller KP, Mongera A, Konantz M, Neuhaus SCF, Nüsslein-Volhard C and Geisler R. S

- lc45a2 and V - ATP ase are regulators of melanosomal p H homeostasis in zebrafish, providing a mechanism for human pigment evolution and disease. *Pigment Cell Melanoma Res*, **26**: 205–217. 2013. <https://doi.org/10.1111/pcmr.12053>, PMID:23205854
- [30] Wiriyasermkul P, Moriyama S and Nagamori S. Membrane transport proteins in melanosomes: regulation of ions for pigmentation. *Biochim Biophys Acta Biomembr*, **1862**: 183318. 2020. <https://doi.org/10.1016/j.bbmem.2020.183318>, PMID:32333855
- [31] Cullinane AR, Vilboux T, O'Brien K, Curry JA, Maynard DM, Carlson-Donohoe H, Ciccone C, Markello TC, Gunay-Aygun M, Huizing M and Gahl WA; NISC Comparative Sequencing Program. Homozygosity mapping and whole-exome sequencing to detect *SLC45A2* and *G6PC3* mutations in a single patient with oculocutaneous albinism and neutropenia. *J Invest Dermatol*, **131**: 2017–2025. 2011. <https://doi.org/10.1038/jid.2011.157>, PMID:21677667
- [32] Kamaraj B and Purohit R. Mutational analysis of oculocutaneous albinism: a compact review. *BioMed Res Int*, **2014**: 905472. 2014. <https://doi.org/10.1155/2014/905472>, PMID:25093188
- [33] Yu S, Wang G, Liao J, Shen X and Chen J. Integrated analysis of long non-coding RNAs and mRNA expression profiles identified potential interactions regulating melanogenesis in chicken skin. *Br Poult Sci*, **64**: 19–25. 2023. <https://doi.org/10.1080/00071668.2022.2113506>, PMID:35979716